SPECTRAL ANALYSIS OF SCOTCH PINE INFESTED BY SIREX NOCTILIO

Nishan Bhattarai, Graduate Student
Lindi J. Quackenbush, Assistant Professor
Laura Calandra, Graduate Student
Jungho Im, Assistant Professor
Stephen Teale, Associate Professor
State University of New York College of Environmental Science and Forestry
Syracuse, NY 13210
nbhattar@syr.edu, ljquack@esf.edu, lncaland@syr.edu, imj@esf.edu, sateale@esf.edu

ABSTRACT

Remote sensing methods for monitoring forest health have advanced with the development of sophisticated new tools and techniques in recent years. Prior research had explored needle-level analysis of Sirex infestation and this research explores a new method of investigating the impact of Sirex woodwasp (*Sirex noctilio*) infestation in Scotch pines using 8-band multispectral WorldView-2 imagery. The goal of the project was to assess if the broadband spectral regions associated with this sensor can characterize subtle changes in spectral reflectance caused by Sirex infestation. Eight different spectral indices were derived from the images and statistical analysis was performed. While the needle-level analysis previously reported showed statistical differences, none of the eight spectral indices showed statistically significant differences between the healthy and infested trees at a 0.05 significance level, though some showed differences with a weaker significance level. An automated calibration model based on exhaustive search techniques was used to consider the optimum threshold to determine the capability of the vegetation index (ices) to detect changes in spectral reflectance from the infested trees. The accuracy assessment results were poor to moderate. The best overall accuracy was 68% with a Kappa coefficient of 0.33. While there is an opportunity to explore multispectral spectral bands of WorldView-2 data in mapping forest health using spectral indices, in our study, the broadband spectral indices were not capable of accurately differentiating the subtle changes in spectral properties of healthy and infested tree at the individual tree level.

KEYWORDS: automated calibration model, forest health, Sirex woodwasp, spectral indices, thresholds

INTRODUCTION

Invasive species are a major challenge to the managing natural resources in many parts of the world. Forests in the northeastern United States are currently under serious environmental and economic threat due to invasion of several invasive forest pests. Sirex woodwasp (*Sirex noctilio*), which is native to Europe, Asia and northern Africa, is a major invasive forest pest in the Northeastern US forests. Though only recently being identified in North America (New York) in 2004 (Hoebeke *et al.*, 2005), Sirex has already drawn increasing interest from scientists and forest managers due to its potential to seriously damage the life cycle of northeastern pines. Sirex has already caused extensive damage to pine forests in Australia, New Zealand, South America, and Africa (Ciesla, 2003). Hence, it is important to mitigate Sirex infestation in the Northeastern US forests to assure pine survival and yield in the area. In order to mitigate potential threats due to Sirex infestation, forest managers need tools and techniques to produce accurate maps showing the spread of the pest.

While traditional approaches for monitoring forest health, such as visual assessment from aerial and/or ground surveys, are important, they are labor and time intensive (Coops *et al.*, 2003). In addition, such approaches are subjected to human biases and are often restricted to visible wavelengths. Remote sensing-based analysis has potential application in invasive species detection and mapping because of the change in spectral reflectance of the canopy that typically corresponds to a decline in condition. The recent advances—in terms of spectral and spatial resolution—of remote sensing technology has increased the potential to provide more efficient processing than traditional approaches in terms of time, labor, and cost.

Satellite imagery with medium spatial and spectral resolution has been widely used in monitoring forest health (e.g., Joria *et al.*, 1991, Luther *et al.*, 1997; Royle and Lathrop, 1997). Previous studies show that broad- and narrow-band vegetation indices, derived from a combination of specific spectral bands, can be used for investigating vegetation health (Gao, 1996; Shafri *et al.*, 2006; Zhao *et al.*, 2005). Royle and Lathrop (2002) used a normalized difference vegetation index (NDVI) derived from multi-temporal Landsat TM/ETM+ images to monitor the health of forest stands infested with hemlock woolly adelgid. Wang *et al.* (2007) used a normalized difference water index (NDWI) derived from Landsat TM images to monitor oak decline in the Ozark Highlands.

Franklin (2001) highlighted the increasing reliance on new data and methods in remote sensing. For forest health studies, there is an opportunity to use remote sensing-based analysis to detect infested trees by deriving new indices that combine specific spectral bands. Hyperspectral images provide many narrow bands and offer the possibility to produce spectral indices that detect subtle changes in spectral reflectance from forest canopy. However, the application of hyperspectral data in regional study is limited due to higher application cost, low coverage area, and limited availability. While use of moderate resolution satellite imagery is cost effective for stand-level analysis, evaluating invasive pest spread in the heterogeneous northeaster forests is often challenging, since most invasive species are host specific. High spatial resolution satellite images, though less cost effective, offers the potential for providing accurate information at the tree level. Efficiently utilizing this data requires consideration of new techniques. The objective of the study is to determine the capability of high resolution multispectral image-derived spectral indices to characterize Sirex-induced stress on pines at a canopy level. The study also aims to explore an automated method of detecting infested trees using spectral indices.

METHODS AND MATERIALS

Study Area and Data

The study area is located in Heiberg Memorial Forest which covers approximately 1600 ha in central New York State (42.75° N, 76.08° W) (Figure 1). The property is managed by the State University of New York College of Environmental Sciences and Forestry (SUNY-ESF). The main tree species in the forest are red maple (*Acer rubrum*), sugar maple (*Acer saccharum*), red oak (*Quercus rubra*), beech varieties (*Fagus*), red pine (*Pinus resinosa*), Scotch pine (*Pinus sylvestris*), Norway spruce (*Picea abies*), eastern hemlock (*Tsuga Canadensis*), and northern white cedar (*Thuja occidentalis*) (Pugh, 2005). Sirex has already been detected in some Scotch pines within Heiberg forest. Studies are being conducted by entomologists from SUNY-ESF to understand the invasion ecology of Sirex in the area.

A WorldView-2 image (DigitalGlobe Inc. 2010) collected on August 7, 2010, was used for the study. The WorldView-2 data contains 8 multispectral bands (2 m spatial resolution) and 1 panchromatic band (0.5 m spatial resolution), though only the multispectral bands were used in this study (Table 1). The image was registered within a 1 pixel RMSE using National Agriculture Imagery Program (NAIP) digital orthoimagery as a reference (NRCS, 2010). The location of healthy and Sirex-infested Scotch pines was collected by two different field crews in the summer and fall of 2009 and 2010 when the infested trees were at early to mid stages of infestation. Locations of the trees were identified in the field using differentially corrected Global Positioning System receivers. Data from 36 infested and 46 healthy trees were used in the analysis. Figure 1 shows the location of the study area and the reference points used in the study.

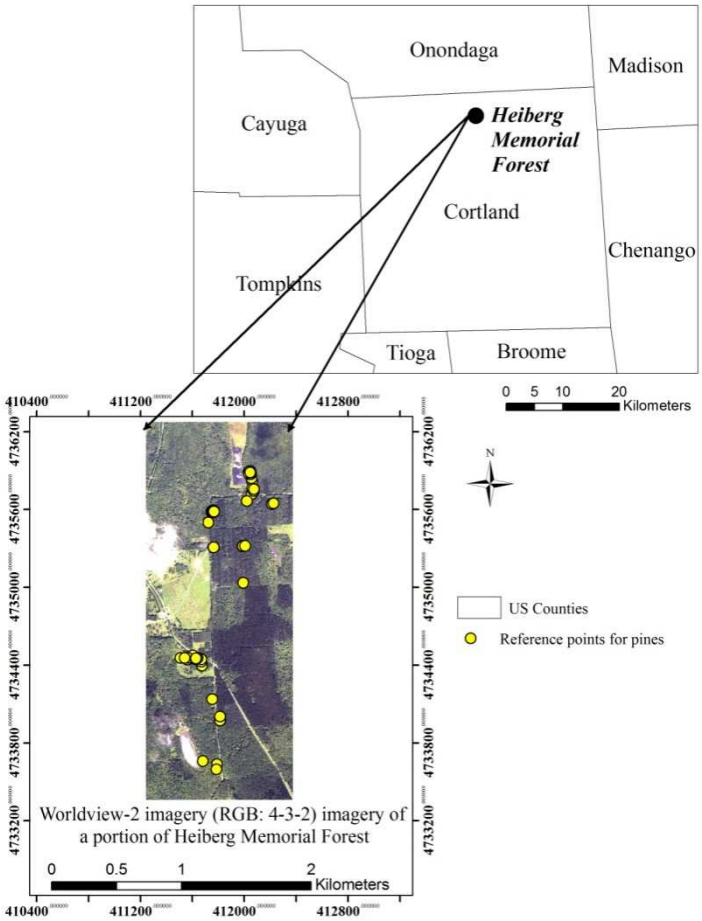

Figure 1. Study area showing location of Scotch pine sampled.

Table 1. WorldView-2 multispectral image bands used

Number	Label	Spectral Range
1	Coastal Blue	400-450 nm
2	Blue	450-510 nm
3	Green	510-580 nm
4	Yellow	585-625 nm
5	Red	630-690 nm
6	Red edge	705-745 nm
7	Near Infrared 1	770-895 nm
8	Near Infrared 2	860-1040 nm

Spectral Indices

Eight different spectral indices were generated in the study. These indices are summarized in Table 2. The band region for each index reported in the original study was best matched to the bandwidth region associated with the WorldView-2 data shown in Table 1. The raw digital numbers (DNs) from the pixel closest to the coordinates of each sampled trees were used to produce the spectral indices.

Table 2. Spectral indices derived from WorldView-2 imagery to investigate Sirex-infested pines

Name	Abb.	Formula used	Reference
Enhanced Vegetation Index *	EVI	$2.5 \times (B_8 - B_5)/(B_8 + 6\times B_8 - 7.5\times B_3 + 1)$	Heute *et al.* (2002)
Modified soil adjusted vegetation index	MSAVI	$\frac{2 \times B_8 + 1 - \sqrt{(2 \times B_8 + 1)^2 - 8(B_8 - B_5)}}{2}$	Qi *et al.* (1994)
Normalized Difference Soil Index	NDSI	$(B_4 - B_3)/(B_4 + B_3)$	Wolf, 2010)
Normalized Difference Vegetation Index	NDVI	$(B_8 - B_5)/ (B_8 + B_5)$	Tucker (1979) and Wolf (2010)
Normalized Difference Water Index	NDWI	$(B_8 - B_1)/(B_8 + B_1)$	(Wolf, 2010)
Non-Homogeneous Feature Difference	NHFD	$(B_6 - B_1)/(B_6 + B_1)$	(Wolf, 2010)
Pigment specific Simple Ratio	PSSR	$(B_7 - B_1)/ (B_7 + B_1)$	Blackburn and Steele (1999)
Structure Insensitive Pigment Index	SIPI	$(B_7 - B_1)/(B_7 + B_5)$	Penuelas *et al.* (1995)

*coefficients from MODIS-EVI were used

Methodology

The methodology flow chart (Figure 2) shows the steps used in this study. The difference in mean spectral indices between healthy and infested pines was tested using two sample t-tests. An automated calibration optimization method (Im *et al.* 2007) was implemented using VBA code in the ESRI ArcGIS 9.3 software to optimize the selection of vegetation indices to separate healthy and infested pines in the study area.

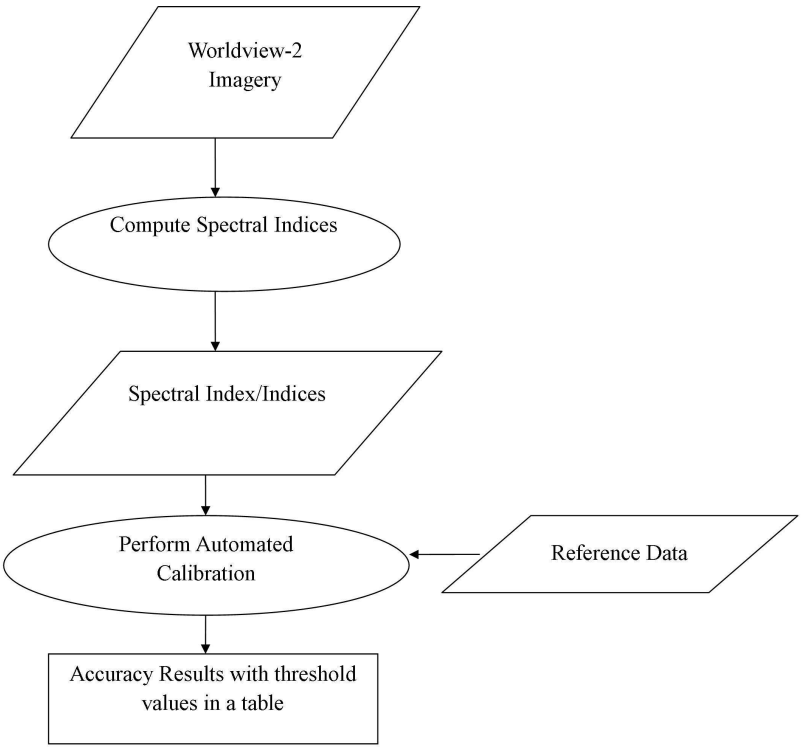

Figure 2. Methodology flowchart.

The automated calibration of the vegetation index thresholds used in this study modifies the automated binary change detection model from Im *et al*. (2007) to separate infested and healthy trees using satellite derived spectral indices. The steps used in the automated model were: (1) user provides threshold parameters (start, end, step size, and threshold type); (2) model automatically extracts index values for each reference point; (3) model automatically computes accuracies for the presence or absence of Sirex for each threshold value or each combination of thresholds when multiple layers are used (i.e., two vegetation indices); (4) export a table showing threshold values and associated overall accuracy, Kappa coefficient, user's and producer's accuracies.

RESULTS AND DISCUSSIONS

Digital Numbers from Healthy and Infested Pines

The DN curves for both healthy and infested tree crowns showed a similar trend (Figure 3). The DN values for all bands were higher in healthy pines with the greatest difference at bands 6, 7, and 8. This indicates that these three bands might be useful in characterizing healthy and infested trees. However, the limited variation in the DN values may indicate that the Sirex-infestation in the forest is at early stages or that infested crowns are partially obscured by healthy trees, generating a mixed response. In later stages of infestation, Sirex causes needle discoloration that would be more apparent in the visible and red-edge bands.

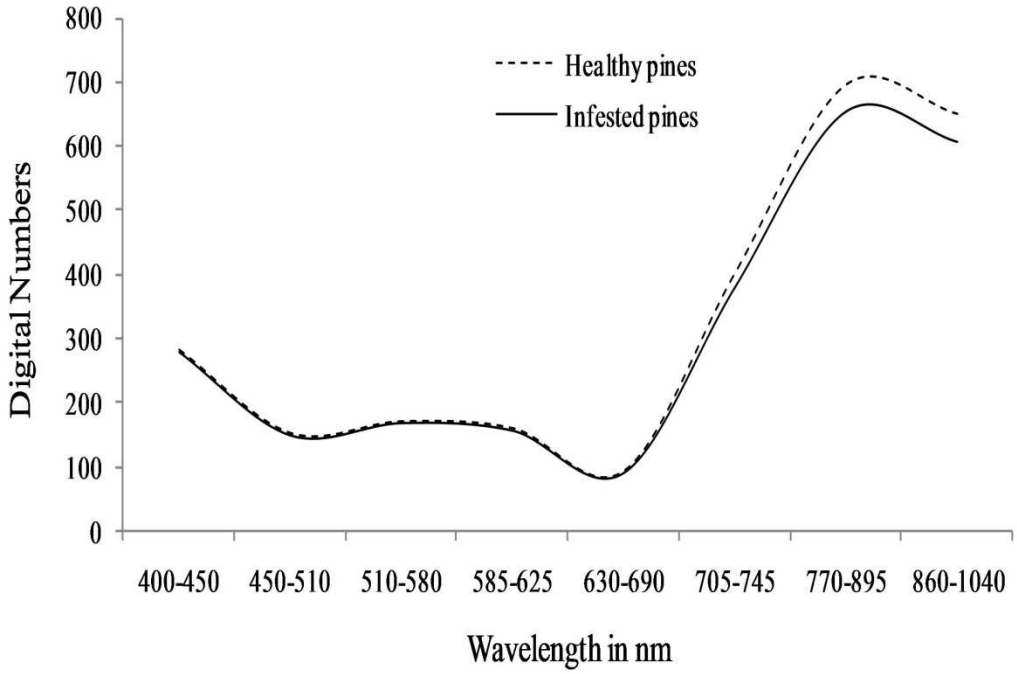

Figure 3. Average DNs for healthy and Sirex-infested pines in WorldView-2 imagery (Aug 7, 2010).

Spectral Indices

Figure 4 shows box plots for the eight spectral indices comparing healthy and infested pines. The box plot indicates that variation in spectral indices is higher in Sirex-infested pines. This variation may correspond to different levels of infestation or tree health. The two sample t-test comparing healthy and Sirex-infested pines for each spectral index showed that the mean difference between vegetation indices was not significant at an α of 0.05 (p-value > 0.05 for all t-tests), though some indices showed differences with a slightly weaker significance level. The p-values from the t-test were: EVI – 0.06, MSAVI – 0.1, NDSI – 0.14, NDVI – 0.09, NDWI – 0.12, NHFD – 0.23, PSSR – 0.16, and SIPI – 0.12.

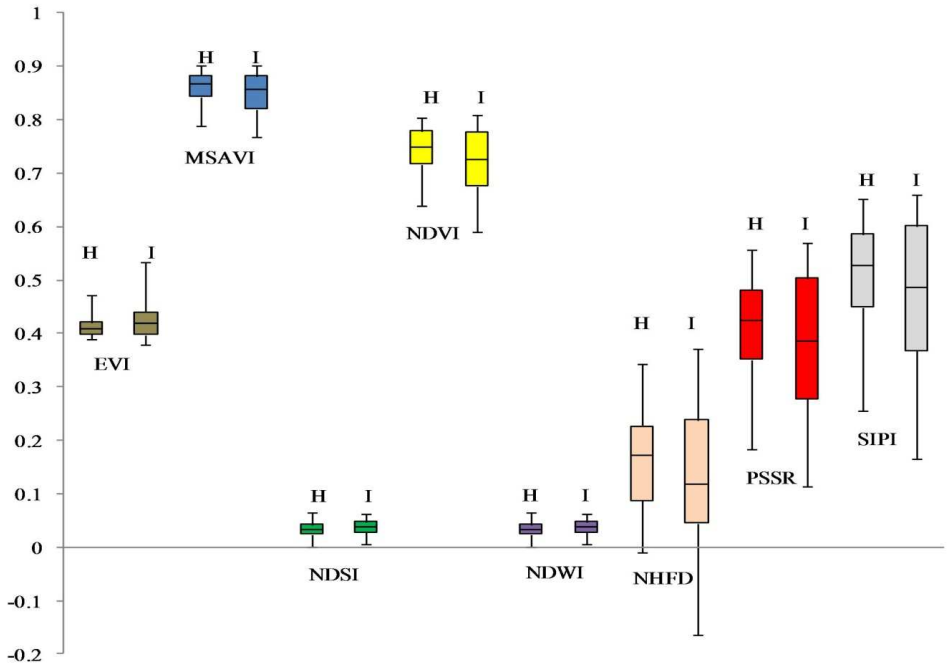

Figure 4. Box plots for different spectral indices from healthy (H) and Sirex-infested (I) trees.

Automated Calibration Model Results

The automatic calibration method using one threshold showed poor to moderate accuracy results (Figure 5), regardless of which index was considered. The best overall accuracy was 68% when NDVI (= 0.69) was used as a threshold. The Kappa values were below 0.33 for all thresholds. The thresholds identified in the automated method were either upper threshold (i.e., pixels below the threshold are classified as Sirex-infested pines) or lower threshold (i.e., pixel above the threshold are classified as Sirex-infested pines). The results from analysis of the spectral indices indicated that the mean of six spectral indices (i.e., MSAVI, NDVI, NDWI, NHFD, PSSR, SIPI) were lower in infested pines, while the other two (EVI and NDSI) were higher in the infested pines. However, the distinction was not significantly different. The results of automated method using one threshold is shown in Figure 5, which indicates that none of the spectral indices used were able to characterize infested and healthy pines crowns with good accuracy. The overall accuracy pattern for all indices was similar. The NDVI threshold produced better results than other thresholds as it was derived from NIR_2 and the red band, which are considered to be most important bands for detecting healthy and invasive plants. However, the poor accuracy results suggest that the NIR bands in the WorldView-2 imagery were not capable of differentiating healthy and Sirex-infested pines in our study.

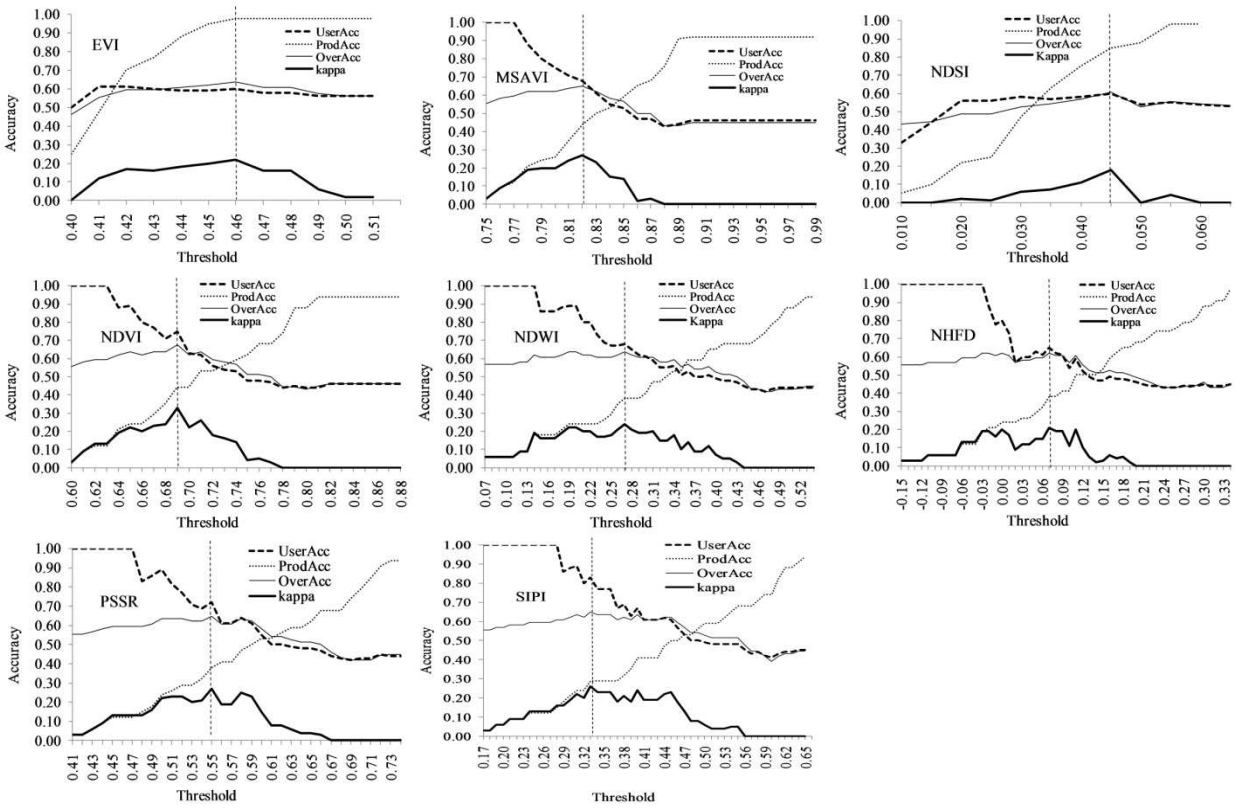

Figure 5. Calibration results using single threshold with user's accuracy, producer's accuracy, overall accuracy, and Kappa statistic, the vertical dashed line shows the best accuracy results at an optimized threshold.

Because NDVI performed the best of the indicators evaluated and has been widely used in monitoring forest health, it was used as a base threshold in automated calibration model with two thresholds. The accuracy results from the automated model using two thresholds (NDVI + one of seven other indices) were similar to the results from the method using single threshold. The maximum overall accuracy obtained was 68% with NDVI (0.69) as one threshold as shown in Table 3. The accuracy results were similar to the results from the automated method using one threshold, as the indices were derived from similar bands and thus are highly correlated.

Table 3. Optimized threshold and best accuracy results from automated calibration with two thresholds

Optimize thresholds	Overall Accuracy	Kappa
EVI (0.39) and NDVI (0.69)	68 %	0.33
MSAVI (0.74) and NDVI (0.69)	68 %	0.33
NDSI (0) and NDVI (0.68)	65 %	0.27
NDWI (0.06) and NDVI (0.69)	68 %	0.33
NHFD (-0.16) and NDVI (0.69)	68 %	0.33
PSSR (0.41) and NDVI (0.69)	68 %	0.33
SIPI (0.24) and NDVI (0.69)	65 %	0.26

Zhang *et al.* (2010) investigated the spectral response of Sirex-infested needles using spectroradiometer measurements observed in the lab and suggested three important spectral regions (i.e., 350–629 nm, 703–1366 nm, and 1883–2033 nm) for comparing the spectral property of healthy and infested scotch pines. They particularly

identified combinations of 377 nm (blue) and 1914 to 1923 nm (NIR) bands; however, these bands are not available in Worldview-2 imagery. The closest bandwidth combination used in the NDWI index combined coastal blue (band 1) and NIR 2 (band 8) did not find statistically significant results. The results from this study suggest that the subtle changes in spectral reflectance of Sirex-infested pines may not be detected from broadband sensors.

The poor accuracy results should not be attributed to the automated calibration model used in this study. Since the mean values of vegetation indices of healthy and infested pines were not significantly different, it was expected that the model would result into poor results. However, there is an opportunity in future to explore the automated process in infested tree detection. The spectral indices supplied in this study may have been highly influenced by other plants which covered Sirex-infested trees at canopy level. The infested trees sampled were widely scattered and Sirex normally attacks pines with suppressed or unhealthy condition. Since these suppressed trees may not reach the canopy level, it is often challenging to extract crown level information for the infested tree using satellite or airborne images. The result of the analysis may have been different if the infested trees were clustered or if the crowns of infested trees were exposed.

SUMMARY AND CONCLUSIONS

Eight spectral indices derived from eight WorldView-2 multispectral bands were analyzed to study the spectral properties of infested and healthy pines. None of the spectral indices from infested and healthy tree were significantly different at significance level of 0.05, though several of the indicators were statistically different with a slightly weaker testing level. An automated calibration method was applied to determine if a vegetation index threshold derived from high resolution satellite imagery could be used to characterize healthy and Sirex-infested trees. However, the accuracy attained from the automated method was poor. Based on the results, it is concluded that spectral bands from WorldView-2 data were not capable of characterizing the subtle changes in spectral reflectance for the Sirex-infested and healthy pine sampled in this study. However, the results were highly influenced by the presence of healthy trees over the canopy of Sirex-infested trees. Hence, mapping Sirex infestation is often challenging. Though high resolution imagery may capture spatial details of each tree on ground, it may not provide better results if the imagery has low spectral resolution. Future study will consider WorldView-2 imagery for characterizing infestation for forests with larger, continuous areas of infestations and compare the results from similar methods using hyperspectral images. Future work will also explore the use of multi-temporal change analysis in characterizing forest health conditions.

REFERENCES

Blackburn G.A. and C.M. Steele, 1999. Towards the remote sensing of matorral vegetation physiology: relationships between spectral reflectance, pigment and biophysical characteristics of semi-arid bushland canopies, *Remote Sensing of Environment*, 70(3): 278-292.

Ciesla, W.M., 2003. European woodwasp, a potential threat to North America's conifer forests. *Journal of Forestry*, 101(2): 18–23.

Coops, N., M. Stanford, M., K. Old, M. Dudzinski, D. Culvenor, and C. Stone, 2003. Assessment of Dothistroma needle blight of *Pinus radiata* using airborne hyperspectral imagery, *Phytopathology*, 93(12): 1524–1532.

de Oliveira, Y.M.M., M.A.D. Rosot, N.B. da Luz, W.M. Ciesla, E.W. Johnson, R. Rhea, and J.F. Penteado Jr., 2006. Aerial Sketchmapping for Monitoring Forest Conditions in Southern Brazil, *Proceeding from RMRS-P-42CD*, September 20-24, 2004, pp. 815-824.

DigitalGlobe Inc., 2010. http://www.digitalglobe.com/index.php/48/Products?product_id=27 (Last accessed on September 27, 2010).

Franklin, S.E., 2001. *Remote Sensing for Sustainable Forest Management*. CRC, Boca Raton, pp. 424.

Gao, B., 1996. NDWI – A normalized difference water index for remote sensing of vegetation liquid water from space, *Remote Sensing of Environment*, 58(3): 257-266.

Hodgson, M. E., X. Li, and Y. Cheng, 2004. A parameterization model for transportation feature extraction, *Photogrammetric Engineering and Remote Sensing*, 70(12): 1399−1404.

Hoebeke, E.R., D.A. Haugen, and R.A. Haack, 2005. *Sirex noctilio*: Discovery of a Palearctic siricid woodwasp in New York, *Newsletter of the Michigan Entomological Society*, 50(1&2):24-25.

Huete, A., K. Didan, T. Miura, E.P. Rodriguez, X. Gao, and L.G. Ferrira, 2002. Overview of the radiometric and biophysical performance of the MODIS vegetation indices, *Remote Sensing of Environment*, 83(2-Jan), 195-213.

Im, J., J. Rhee, J.R. Jensen, and M.E. Hodgson, 2007. An automated binary change detection model using a calibration approach, *Remote Sensing of Environment*, 106(2007): 89-105.

Joria, P.E., S.C. Ahearn, and M. Connor, 1991. A comparison of the SPOT and Landsat Thematic Mapper satellite systems for detecting gypsy moth defoliation in Michigan, *Photogrammetric Engineering and Remote Sensing*, 57(12): 1605–1612.

Luther, J.E., S.E. Franklin, J. Hudak, and J.P. Meades, 1997. Forecasting the susceptibility and vulnerability of balsam fir stands to insect defoliation with Landsat Thematic Mapper data, *Remote Sensing of Environment*, 59(1): 77–91.

Natural Resources Conservation service (NRCS), 2010. http://datagateway.nrcs.usda.gov/GDGOrder.aspx (Last accessed on December 10, 2010).

Penuelas J., I. Feilla, P. Lloret, F. Munoz, and M. Vilajeliu, 1995. Reflectance assessment of mite effects on apple trees, *International Journal of Remote Sensing*, 16(14): 2727–2733.

Pugh, M.L., 2005. Forest terrain feature characterization using multi-sensor neural image fusion and feature extraction methods. Ph.D. Dissertation, State University of New York College of Environmental Science and Forestry, pp. 215.

Qi J., Y. Kerr, and A. Chehbouni, 1994. External factor consideration in vegetation index development, *Proceedings of Physical Measurements and Signatures in Remote Sensing*, International Society for Photogrammetry and Remote Sensing, pp.723-730.

Royle, D.D., and R.G. Lathrop, 1997. Monitoring hemlock forest health in New Jersey using Landsat TM data and change detection techniques, *Forest Science*, 43(3): 327–335.

Royle, D.D., and R.G. Lathrop, 2002. Discriminating *Tsuga canadensis* hemlock forest defoliation using remotely sensed change detection, *Journal of Nematology*, 34(3): 213–221.

Shafri, H.Z.M., M.A.M. Salleh, and A. Ghiyamat, 2006. Hyperspectral remote sensing of vegetation using red edge position techniques, *American Journal of Applied Sciences*, 3(6): 1846-1871.

Stehman, S.V., 1999. Comparing thematic maps based on map value, *International Journal of Remote Sensing*, 20(12): 2347–2366.

Tucker, C. J., 1979. Red and photographic infrared linear combinations for monitoring vegetation, *Remote Sensing of Environment*, 8(2): 127-150.

Wang, C., Z. Lu, and T.L., Haithcoat, 2007. Using Landsat images to detect oak decline in the Mark Twain National Forest, Ozark Highlands, *Forest ecology and management*, 240(1-3): 70–78.

Wolf, A., 2010. Using WorldView 2 Vis-NIR MSI Imagery to Support Land Mapping and Feature Extraction Using Normalized Difference Index Ratios, submitted for Digital Globe 8-Band Challenge, http://www.digitalglobe.com/downloads/8bc/WorldView-2_8-Band_Challenge_-_Antonio_Wolf.pdf (Last accessed on February 10, 2011).

Zhang, W., L. Calandra, L.J. Quackenbush, J. Im, and S.A. Teale, 2010. Monitoring Scotch pine infested by *Sirex noctilio* using hyperspectral data: a laboratory study. Proceedings, ASPRS Annual Conference, San Diego, CA, 28–30 April, unpaginated CD-ROM.

Zhao, D.H., J.L. Li, and J.G. Qi, 2005. Identification of red and NIR spectral regions and vegetation indices for discrimination of cotton nitrogen stress and growth stage, *Computers and Electronics in Agriculture*, 48(2): 155-169.